Precipitating Quasigeostrophic Equations and Potential Vorticity Inversion with Phase Changes

LESLIE M. SMITH

Department of Mathematics, and Department of Engineering Physics, University of Wisconsin–Madison, Madison, Wisconsin

SAMUEL N. STECHMANN

Department of Mathematics, and Department of Atmospheric and Oceanic Sciences, University of Wisconsin–Madison, Madison, Wisconsin

(Manuscript received 24 January 2017, in final form 3 July 2017)

ABSTRACT

Precipitating versions of the quasigeostrophic (QG) equations are derived systematically, starting from the equations of a cloud-resolving model. The presence of phase changes of water from vapor to liquid and vice versa leads to important differences from the dry QG case. The precipitating QG (PQG) equations, in their simplest form, have two variables to describe the full system: a potential vorticity (PV) variable and a variable M including moisture effects. A PV-and-M inversion allows the determination of all other variables, and it involves an elliptic partial differential equation (PDE) that is nonlinear because of phase changes between saturated and unsaturated regions. An example PV-and-M inversion is provided for an idealized cold-core cyclone with two vertical levels. A key point illustrated by this example is that the phase interface location is unknown a priori from PV and M, and it is discovered as part of the inversion process. Several choices of a moist PV variable are discussed, including subtleties that arise because of phase changes. Boussinesq and anelastic versions of the PQG equations are described, as well as moderate and asymptotically large rainfall speeds. An energy conservation principle suggests that the model has firm physical and mathematical underpinnings. Finally, an asymptotic analysis provides a systematic derivation of the PQG equations, which arise as the limiting dynamics of a moist atmosphere with phase changes, in the limit of rapid rotation and strong stratification in terms of both potential temperature and equivalent potential temperature.

1. Introduction

Quasigeostrophic (QG) equations have been an invaluable tool for understanding midlatitude atmospheric dynamics. They provide a simplified setting for understanding a variety of phenomena, such as baroclinic instability (Charney 1947, 1948; Eady 1949; Phillips 1954) and geostrophic turbulence (Charney 1971; Rhines 1979; Salmon 1980), to name a few.

In their traditional form, the QG equations do not include moisture, precipitation, or latent heat release. Nevertheless, a moist QG framework can be useful as a simplified setting for investigating moisture and its effects on midlatitude dynamics. In one type of approach (e.g., Lapeyre and Held 2004; Monteiro and Sukhatme 2016), one can build a moist QG framework by supplementing the dry QG equations with a moisture variable and convective parameterization. In other QG frameworks (Mak 1982; Bannon 1986; Emanuel et al. 1987; De Vries et al. 2010), the dry QG equations have been supplemented by parameterizations of latent heating without explicitly incorporating the dynamics of a moisture variable. These formulations are sensible in terms of their simplicity. However, in these formulations, the moist component of the model is treated somewhat as a supplement. As a result, a remaining question is, Can a moist QG model be derived as the limit, under rapid rotation and strong (moist) stratification, of the comprehensive dynamics of a moist atmosphere? If so, then what is the form of such a moist QG model, and what are its main properties?

The main goals of the present paper are 1) to systematically derive a precipitating quasigeostrophic (PQG) model, starting from the equations of a cloud-resolving model (CRM) and 2) to take first steps toward

Corresponding author: Samuel N. Stechmann, stechmann@wisc.edu

DOI: 10.1175/JAS-D-17-0023.1

understanding the properties of the PQG system. One important property of the PQG system is an energy conservation principle. Another important property is its formulation in terms of a potential vorticity (PV) variable and a second variable M that accounts for moisture effects. From these two variables, in the simplest version of the PQG equations, a PV-and-M inversion problem allows all other variables to be determined, including moisture. The PV-and-M inversion is formulated as an elliptic partial differential equation (PDE) with nonlinearity entering through the effects of phase changes. To illustrate the PV-and-M inversion process and its key differences from dry QG, an example with an idealized, axisymmetric, cold-core cyclone is presented. One interesting property of PV-and-M inversion is that the phase boundaries are unknown a priori and are discovered as part of the inversion process.

In the future, it would be interesting to use the PQG model to investigate both the hydrological cycle and the effects of latent heat release on midlatitude dynamics. As one step in these directions, meridional moisture transport is studied in a linear analysis by Wetzel et al. (2017, manuscript submitted to *Math. Climate Wea. Forecasting*), and the effects of precipitation are seen to impact the vertical structure of meridional moisture flux. Many other questions could also potentially benefit from the simplified viewpoint provided by the PQG equations, including questions on the hydrological cycle (Peixoto and Oort 1992; Trenberth and Stepaniak 2003; Frierson et al. 2006; Held and Soden 2006; Schneider et al. 2010; Laliberté et al. 2012; Newman et al. 2012; Shaw and Pauluis 2012) and the effects of latent heating on extratropical cyclones and eddies (Davis 1992; Posselt and Martin 2004; Brennan and Lackmann 2005; O'Gorman 2011; Pfahl et al. 2015). For example, the PQG model could potentially provide insight into the appropriate effective static stability for a moist atmosphere (e.g., Lapeyre and Held 2004; O'Gorman 2011).

The remainder of the manuscript is organized as follows. In section 2, we describe the CRM used as the starting point for the PQG analysis and introduce notation. Section 3 presents the main ideas underlying the PQG model derivation. A comparison with other prior moist midlatitude models is also presented. Section 4 introduces 1) the moist potential vorticity PV_e based on equivalent potential temperature and 2) the new dynamical variable M, which is a linear combination of equivalent potential temperature θ_e and total water mixing ratio q_t. The nonlinear elliptic equation for a PV_e-and-M inversion is also derived and discussed. In section 5, the energy conservation principle is presented and decomposed into four contributions: kinetic, unsaturated potential, saturated potential, and moist potential. Section 6 briefly describes the changes that occur if the rainfall speed is asymptotically large instead of order one. Alternate choices of potential vorticity are discussed in section 7. A semianalytic solution for an idealized, axisymmetric, cold-core cyclone is used in section 8 to illustrate the PV-and-M inversion, as well as determination of phase boundaries in this simple case. Section 9 describes extension of the approach to an anelastic atmosphere and more general cloud microphysics, and concluding remarks are given in section 10. The systematic asymptotic derivation of the PQG equations is recorded in the appendix, including nondimensionalization of the equations, the precise distinguished limit, and asymptotic expansion.

2. Starting point: Cloud-resolving model and cloud microphysics

For the cloud-resolving model and cloud microphysics, we break the paper into two parts. First, in this section and in most of the paper, we work with an idealized CRM (Hernandez-Duenas et al. 2013). Second, in section 9, we describe the generalization to other versions of cloud microphysics. The idealized CRM is considered first, since it includes many of the essential features of other versions of cloud microphysics and since it allows the PV-and-M inversion to be written in concrete form (section 4) as opposed to the more complicated formulation presented in section 9.

In this section, as our starting point for the dynamics of a precipitating atmosphere, we describe an idealized CRM with a minimal version of cloud microphysics. The model was designed and analyzed by Hernandez-Duenas et al. (2013) and called the fast autoconversion and rain evaporation (FARE) model.

The inviscid FARE system is

$$\frac{D\mathbf{u}}{Dt} + f\hat{\mathbf{z}} \times \mathbf{u} = -\nabla\left(\frac{p}{\rho_o}\right) + \hat{z}\,b, \tag{1a}$$

$$\nabla \cdot \mathbf{u} = 0, \tag{1b}$$

$$\frac{D\theta_e}{Dt} + w\frac{d\tilde{\theta}_e}{dz} = 0, \quad \text{and} \tag{1c}$$

$$\frac{Dq_t}{Dt} + w\frac{d\tilde{q}_t}{dz} - V_T\frac{\partial q_r}{\partial z} = 0. \tag{1d}$$

The dynamical variables are the velocity $\mathbf{u} = (u, v, w)$, pressure p, equivalent potential temperature anomaly θ_e, and anomalous mixing ratio of total water q_t, all of which are functions of the three-dimensional spatial coordinate $\mathbf{x} = (x, y, z)$ and time t. The buoyancy b may be expressed as a function of θ_e and q_t and z as described below. Using standard notation, $D/Dt = \partial/\partial t + \mathbf{u} \cdot \nabla$ is the material derivative, f is the Coriolis parameter, and V_T is the fall speed of rain, taken to be a constant value here for simplicity. All thermodynamic variables have been decomposed into background functions of altitude and anomalies. For example, the total equivalent potential temperature is $\theta_e^{\mathrm{tot}}(\mathbf{x}, t) = \tilde{\theta}_e(z) + \theta_e(\mathbf{x}, t)$, where $\tilde{\theta}_e(z)$ is the background state. Similarly, the mixing ratio of water is $q_t^{\mathrm{tot}}(\mathbf{x}, t) = \tilde{q}_t(z) + q_t(\mathbf{x}, t)$. Though we will use constant $d\tilde{q}_t/dz$ and $d\tilde{\theta}_e/dz$ herein, extension to nonconstant slopes is straightforward. Note that (1) has been written using the Boussinesq approximation with constant density ρ_o; an analogous anelastic model is described in section 9.

The total water q_t^{tot} is the sum of contributions from water vapor q_v^{tot} and rainwater q_r^{tot}:

$$q_t^{\mathrm{tot}} = q_v^{\mathrm{tot}} + q_r^{\mathrm{tot}}. \tag{2}$$

Note that condensed cloud water q_c^{tot}, which is commonly included in bulk cloud microphysics schemes (e.g., Kessler 1969; Grabowski and Smolarkiewicz 1996), is not included in the FARE model; this is due to the assumption of fast autoconversion of smaller liquid droplets q_c^{tot} to larger rain drops q_r^{tot}. A second assumption of the FARE model is fast rain evaporation: if rain falls into unsaturated air, it immediately either evaporates all rain or evaporates just enough rain to reach saturation. As a result, the water vapor and rainwater can be recovered from q_t^{tot} using

$$q_v^{\mathrm{tot}} = \min(q_t^{\mathrm{tot}}, q_{vs}^{\mathrm{tot}}), \quad q_r^{\mathrm{tot}} = \max(0, q_t^{\mathrm{tot}} - q_{vs}^{\mathrm{tot}}), \tag{3}$$

where q_{vs}^{tot} is the saturation mixing ratio. Again for simplicity, the FARE model adopts a prescribed saturation mixing ratio profile depending only on altitude: $q_{vs}^{\mathrm{tot}}(z)$. This is an approximation $q_{vs}^{\mathrm{tot}}(p^{\mathrm{tot}}, T^{\mathrm{tot}}) \approx q_{vs}^{\mathrm{tot}}[\tilde{p}(z), \tilde{T}(z)]$ of the standard Clausius–Clapeyron relation assuming that the total thermodynamic variables p^{tot} and T^{tot} are close to the background state values $\tilde{p}$ and $\tilde{T}$ (Majda et al. 2010; Deng et al. 2012; Hernandez-Duenas et al. 2013).

Linearized thermodynamics have been used to derive (1), and in particular, the equivalent potential temperature is here defined as

$$\theta_e^{\mathrm{tot}} \equiv \theta^{\mathrm{tot}} + \frac{L_v}{c_p} q_v^{\mathrm{tot}}, \tag{4}$$

which is a linearization of the standard definition $\theta_e^{\mathrm{tot}} = \theta^{\mathrm{tot}} \exp[(L_v q_v^{\mathrm{tot}})/(c_p T^{\mathrm{tot}})]$, where the latent heat factor $L_v \approx 2.5 \times 10^6\,\mathrm{J\,kg^{-1}}$ and specific heat $c_p \approx 10^3\,\mathrm{J\,kg^{-1}\,K^{-1}}$. [Note that this linearized equivalent potential temperature is similar to the moist entropy, which has been used in other simplified models, e.g., the two-layer model of Lambaerts et al. (2011).] The potential temperature θ^{tot} can be recovered from θ_e^{tot} and q_t^{tot} using

$$\theta^{\mathrm{tot}} = \begin{cases} \theta_e^{\mathrm{tot}} - \dfrac{L_v}{c_p} q_t^{\mathrm{tot}} & \text{if} \quad q_t^{\mathrm{tot}} < q_{vs}^{\mathrm{tot}}(z) \\ \theta_e^{\mathrm{tot}} - \dfrac{L_v}{c_p} q_{vs}^{\mathrm{tot}}(z) & \text{if} \quad q_t^{\mathrm{tot}} \ge q_{vs}^{\mathrm{tot}}(z) \end{cases}, \tag{5}$$

which combines (3) and (4). This will be useful, for instance, in defining the buoyancy as a function of θ_e and q_t below.

In what follows, the anomalies θ_e, q_t, etc., will primarily be used rather than the total thermodynamic variables θ_e^{tot}, q_t^{tot}, etc. Considering an unsaturated background state, the relationships in (2)–(5) will hold in the same form with the superscript "tot" removed, provided that one decomposes q_{vs}^{tot} as

$$q_{vs}^{\mathrm{tot}}(z) = \tilde{q}_{vs}(z) + q_{vs}(z), \tag{6}$$

with the choice of

$$\tilde{q}_{vs}(z) = \tilde{q}_v(z) = \tilde{q}_t(z), \tag{7}$$

and

$$\tilde{q}_r(z) = 0. \tag{8}$$

In essence, this choice of $\tilde{q}_{vs}$ allows one to write the saturation condition $q_t^{\mathrm{tot}} = q_{vs}^{\mathrm{tot}}$ in the same form in terms of anomalies: $q_t = q_{vs}$. As a result, in terms of the anomalies, (2)–(5) become

$$q_t = q_v + q_r, \tag{9}$$

$$q_v = \min(q_t, q_{vs}), \quad q_r = \max(0, q_t - q_{vs}), \tag{10}$$

$$\theta_e = \theta + \frac{L_v}{c_p} q_v, \quad \text{and} \tag{11}$$

$$\theta = \begin{cases} \theta_e - \dfrac{L_v}{c_p} q_t & \text{if} \quad q_t < q_{vs}(z) \\ \theta_e - \dfrac{L_v}{c_p} q_{vs}(z) & \text{if} \quad q_t \ge q_{vs}(z). \end{cases} \tag{12}$$

Note that adoption of a saturated background state would change the relations between the anomalies and some details of the analysis presented below (Wetzel et al. 2017, manuscript submitted to *Math. Climate Wea. Forecasting*).

The buoyancy b is commonly written in terms of potential temperature θ, water vapor q_v, and rainwater q_r:

$$b = g\left(\frac{\theta}{\theta_o} + R_{vd} q_v - q_r\right), \tag{13}$$

with constant background potential temperature $\theta_o \approx 300\,\mathrm{K}$, gravitational acceleration $g \approx 9.8\,\mathrm{m\,s^{-2}}$, and $R_{vd} = (R_v/R_d) - 1 \approx 0.61$ involving the ratio of gas constants R_v, R_d for water vapor and dry air, respectively.

Alternatively, one may write the buoyancy as a function of θ_e, q_t, and z, with a functional form that changes depending on whether the phase is unsaturated or saturated. More specifically, (13) can be written as

$$b = b_u H_u + b_s H_s, \tag{14}$$

where H_u and H_s are Heaviside functions that indicate the unsaturated and saturated phases, respectively, and are therefore functions of q_t and $q_{vs}(z)$:

$$H_u = \begin{cases} 1 & \text{for} \quad q_t < q_{vs}(z) \\ 0 & \text{for} \quad q_t \geq q_{vs}(z) \end{cases}, \tag{15}$$

and

$$H_s = 1 - H_u. \tag{16}$$

Following from (9)–(13), the variables b_u and b_s are given by

$$b_u = g\left[\frac{\theta_e}{\theta_o} + \left(R_{vd} - \frac{L_v}{c_p\theta_o}\right)q_t\right] \quad \text{and} \tag{17a}$$

$$b_s = g\left[\frac{\theta_e}{\theta_o} + \left(R_{vd} - \frac{L_v}{c_p\theta_o} + 1\right)q_{vs}(z) - q_t\right], \tag{17b}$$

and are both defined in unsaturated and saturated regions alike. Since $R_{vd} \approx 0.61$ and $L_v/(c_p\theta_o) = O(10)$, the coefficients $[R_{vd} - L_v/(c_p\theta_o)]$ and $[R_{vd} - L_v/(c_p\theta_o) + 1]$ are both negative, and thus, the buoyancies are both smaller than $g\theta_e/\theta_o$. Dry and moist buoyancy variables such as in (14) and (17) have also been utilized in studies of nonprecipitating moist convection (Kuo 1961; Bretherton 1987; Pauluis and Schumacher 2010). The formulations (14)–(17) will be convenient in what follows because they separate the continuous functional dependence within b_u and b_s from the discontinuous nature of the phase change within H_u and H_s.

The FARE model has some features that make it an advantageous option of an idealized CRM. The model is similar to some earlier models (Seitter and Kuo 1983; Emanuel 1986; Majda et al. 2010; Deng et al. 2012), which all utilize an assumption of fast autoconversion. A distinguishing feature of the FARE model of Hernandez-Duenas et al. (2013) is that the evaporation of rain occurs instantaneously in unsaturated air, in contrast to the finite rain evaporation time scales used by earlier models (Seitter and Kuo 1983; Emanuel 1986; Majda et al. 2010; Deng et al. 2012). One can view this as an assumption that all, not some, of these microphysical time scales are fast relative to the dynamical time scale of interest. Also, the FARE model of Hernandez-Duenas et al. (2013) has a well-defined energy principle. In prior results, the FARE model was shown to reproduce the basic regimes of precipitating turbulent convection: scattered convection in an environment of low wind shear and a squall line in an environment with strong wind shear (Hernandez-Duenas et al. 2013). These prior results suggest that the FARE model encompasses an adequate representation of cloud microphysics, even though its form is highly simplified.

3. Derivation of the precipitating QG model

In this section, a PQG model is derived from the idealized CRM in (1). (Note that PQG models can also be derived from other CRMs with other cloud microphysics, as described later in section 9. The present section provides the main ideas for the more general derivations as well.) In what follows, we give the ideas and derivation steps briefly and draw attention to the differences from the dry case. In the appendix, we present the systematic perturbation expansion approach based on a distinguished limit.

As for dry QG, a main assumption is that appropriately defined Rossby and Froude numbers are comparable and small. A key new assumption will be that $d\tilde{\theta}_e/dz$ is large and $-(L_v/c_p)d\tilde{q}_t/dz$ may be the same order of magnitude (with $d\tilde{q}_t/dz < 0$). In nature, the assumption of large $d\tilde{\theta}_e/dz$ is valid in much of the extratropics in the zonal mean (e.g., Peixoto and Oort 1992), and it also holds locally at many longitudes; however, locally in some regions, such as in the vicinity of fronts, assumptions of strong moist stratification and/or classical QG scaling may not hold.

Considering large horizontal scales at midlatitudes, with a strongly stable stratification, one could expect the dominant terms in (1) to satisfy a geostrophic, hydrostatic balance:

$$f\hat{\mathbf{z}} \times \mathbf{u}_h = -\nabla_h\phi, \quad b_u H_u + b_s H_s = \frac{\partial\phi}{\partial z}, \tag{18}$$

where $\phi = p/\rho_o$, $\mathbf{u}_h = (u, v)$ is the horizontal wind and $\nabla_h = \hat{\mathbf{x}}\partial/\partial x + \hat{\mathbf{y}}\partial/\partial y$ is the horizontal gradient operator. The leading-order vertical velocity is zero, since the lone dominant term in (1c) is $w(d\tilde{\theta}_e/dz)$ and we have assumed large $d\tilde{\theta}_e/dz$. Thus, the horizontal wind determined from (18) satisfies an incompressibility condition $\nabla_h \cdot \mathbf{u}_h = 0$. Upon defining the streamfunction $\psi = \phi/f$, the resulting diagnostic equations may be written as

$$u=-\frac{\partial\psi}{\partial y},\quad v=\frac{\partial\psi}{\partial x},\quad \zeta=\nabla_h^2\psi\quad\text{and}\tag{19a}$$

$$b_uH_u+b_sH_s=f\frac{\partial\psi}{\partial z},\tag{19b}$$

where ζ is the vertical component of the vorticity. The leading-order form of the buoyancy is proportional to θ,

$$b=g\frac{\theta}{\theta_o},\tag{20}$$

and hence, the diagnostic relation [(19b)] looks similar to the standard dry QG formulation, except it includes important phase-change information. To appreciate the latter, recall that both temperature θ and buoyancy b change their functional form in different phases according to (12) and the asymptotic form of (17):

$$b_u=g\left(\frac{\theta_e}{\theta_o}-\frac{L_v}{c_p\theta_o}q_t\right)\quad\text{and}\tag{21a}$$

$$b_s=g\left[\frac{\theta_e}{\theta_o}-\frac{L_v}{c_p\theta_o}q_{vs}(z)\right].\tag{21b}$$

Proceeding to include next-order corrections to the diagnostic relations [(19)], one finds the equations

$$\frac{D_h\zeta}{Dt}=f\frac{\partial w}{\partial z},\tag{22a}$$

$$\frac{D_h\theta_e}{Dt}+w\frac{d\tilde{\theta}_e}{dz}=0,\quad\text{and}\tag{22b}$$

$$\frac{D_hq_t}{Dt}+w\frac{d\tilde{q}_t}{dz}=V_T\frac{\partial q_r}{\partial z}.\tag{22c}$$

involving the small vertical velocity w, where $D_h/Dt=\partial/\partial t+\mathbf{u}_h\cdot\nabla_h$. Relation (22a) between the lowest-order vorticity and the vertical velocity results from combining next-order corrections in the horizontal momentum balance of (1a) and the incompressibility constraint [(1b)]. Starting from (1c), the balance [(22b)] is consistent with large (positive) $d\tilde{\theta}_e/dz$ and small vertical velocity such that $w\,d\tilde{\theta}_e/dz$ balances horizontal advection of the anomaly θ_e. Similarly, (22c) suggests relatively large $|d\tilde{q}_t/dz|$, such that $w\,d\tilde{q}_t/dz$ balances horizontal advection of anomaly q_t and the rainfall term.

Together, (21) and (22) compose a formulation of the PQG approximation. The main differences from dry QG are the phase changes in the hydrostatic balance and the need for two thermodynamic variables (e.g., θ_e and q_t, instead of one, e.g., θ). In the next sections, the nature of the phase change is described in more detail in the context of potential vorticity, potential vorticity inversion, and energetics.

To compare this PQG system to other prior moist midlatitude systems, consider the form of the latent heating in the PQG system:

$$\frac{D_h\theta}{Dt}+w\frac{d\tilde{\theta}}{dz}=\begin{cases}0 & \text{if}\quad q_t<q_{vs}(z)\\ -\dfrac{L_v}{c_p}\dfrac{d\tilde{q}_{vs}(z)}{dz}w & \text{if}\quad q_t\ge q_{vs}(z),\end{cases}\tag{23}$$

which follows from the PQG system in (22b) and (22c) and the definition of θ in terms of θ_e and q_t in (12). The trigger for the latent heating here is the condition $q_t\ge q_{vs}(z)$, which is similar to convective adjustment models (e.g., Lapeyre and Held 2004; Dias and Pauluis 2010; Lambaerts et al. 2012; Monteiro and Sukhatme 2016) but different from wave–conditional instability of the second kind (CISK) convective parameterizations and others (e.g., Mak 1982; Bannon 1986; Emanuel et al. 1987; De Vries et al. 2010), which utilize vertical velocity or horizontal convergence to define the trigger. For the closure of latent heating, on the other hand, these similarities are somewhat reversed. The closure for the latent heating here is $-(L_v/c_p)(d\tilde{q}_{vs}/dz)w$, which is proportional to vertical velocity w, somewhat similar to wave–CISK closures but different from convective adjustment models where heating is related to the water content such as q_t-q_{vs}. Despite some of these similarities in form, notice that the PQG system here is derived under the assumption of quasigeostrophic scaling in the absence of convection. In contrast, many prior moist QG systems describe the latent heating as a convective parameterization arising from unresolved convection. It would be interesting to incorporate the effects of subsynoptic-scale convection into the PQG system in a systematic way in the future. The present PQG system allows a simpler form for the investigation of the effects of phase changes in a QG system.

We close this section by noting that one might choose to work with the buoyancies (b_u, b_s) instead of (θ_e, q_t) by combining (22b) and (22c). The algebra leads to the equivalent PQG system

$$\frac{D_h\zeta}{Dt}=f\frac{\partial w}{\partial z},\tag{24a}$$

$$\frac{D_hb_u}{Dt}+N_u^2w=-\frac{gL_v}{\theta_oc_p}V_T\frac{\partial q_r}{\partial z},\quad\text{and}\tag{24b}$$

$$\frac{D_hb_s}{Dt}+N_s^2w=0,\tag{24c}$$

where the asymptotic forms of the buoyancy frequencies are

$$N_u^2 = \frac{g}{\theta_o}\frac{d}{dz}\left(\tilde{\theta}_e - \frac{L_v}{c_p}\tilde{q}_v\right) = \frac{g}{\theta_o}\frac{d\tilde{\theta}}{dz} \quad \text{and} \tag{25a}$$

$$N_s^2 = \frac{g}{\theta_o}\frac{d\tilde{\theta}_e}{dz}. \tag{25b}$$

For consistency between (24) and (25) and their original non-QG versions, the asymptotic form of N_s^2 in (25b) requires an additional assumption of $|dq_{vs}/dz| \ll |d\tilde{q}_{vs}/dz|$ (see the appendix). One advantage of the formulation in (24) is that b_u and b_s are related to ψ_z in a simple way, from hydrostatic balance, which will be utilized below.

4. Formulation in terms of two dynamical variables: PV and *M*

Next, we describe how the vertical velocity w can be eliminated from the PQG system in (22). As in the case of dry QG dynamics, this will involve the definition of a PV variable. In addition, here in the case of PQG dynamics, a second variable M is also needed in order to account for moisture. Then, given both a PV and M, one can recover any other variable through PV-and-M inversion.

a. A definition of potential vorticity

To eliminate the vertical velocity w from the vorticity equation in (22a), one option is to combine it with the equivalent potential temperature equation in (22b). (See section 7 below for other options.) The appropriate combination is the following definition of potential vorticity:

$$\mathrm{PV}_e \equiv \zeta + \frac{f}{B_e}\frac{\partial\theta_e}{\partial z}, \tag{26}$$

where $B_e = d\tilde{\theta}_e/dz$. The evolution equation for PV_e can be found by combining (22a) and (22b):

$$\frac{D_h\mathrm{PV}_e}{Dt} = -\frac{f}{B_e}\frac{\partial\mathbf{u}_h}{\partial z}\cdot\nabla_h\theta_e. \tag{27}$$

Notice that the right-hand side of this equation is nonzero, and hence, PV_e is not a material invariant.

b. A definition of the variable M

To eliminate the vertical velocity w from the thermodynamic evolution equations, notice from (22) that a convenient combination of θ_e and q_t is the new anomalous quantity

$$M = q_t + G_M\theta_e, \quad G_M = -\frac{d\tilde{q}_t/dz}{d\tilde{\theta}_e/dz}, \tag{28}$$

where M has units of a water mixing ratio. Multiplying (22b) by G_M and adding the result to (22c) leads to

$$\frac{D_hM}{Dt} = V_T\frac{\partial q_r}{\partial z}. \tag{29}$$

Hence, the variable M is transported horizontally, unaffected by vertical velocity, and is conserved in unsaturated regions but altered by falling rainwater in saturated regions.

Note that this variable M is similar to a variable called Z that has been used in prior studies (Frierson et al. 2004; Stechmann and Majda 2006; Majda and Stechmann 2011; Chen and Stechmann 2016).

c. Summary of dynamics in terms of PV_e *and M*

To summarize, by eliminating the vertical velocity w, the PQG dynamics in (22) has been rewritten in terms of the two variables PV_e and M. Their evolution equations, from (27) and (29), are

$$\frac{D_h\mathrm{PV}_e}{Dt} = -\frac{f}{B_e}\frac{\partial\mathbf{u}_h}{\partial z}\cdot\nabla_h\theta_e \quad \text{and} \tag{30}$$

$$\frac{D_hM}{Dt} = V_T\frac{\partial q_r}{\partial z}. \tag{31}$$

Notice the difference from dry QG theory. In dry QG theory, the entire dynamics can be described in terms of a single variable: the potential vorticity. In the PQG system, in contrast, the moist variable M is also needed.

The eigenmodes of the linearized FARE system suggest that the variables PV and M are natural choices for describing the PQG system: PV represents the amplitude of the vortical mode, and M represents the amplitude of the additional eigenmode that arises when moisture is added to dry dynamics (e.g., Hernandez-Duenas et al. 2015). The vortical mode is a nonpropagating (zero frequency) mode, and the M mode is nonpropagating (zero frequency) when $V_T = 0$. Therefore, PV and M represent the slow or low-frequency eigenmodes, as described by the quasigeostrophic approximation, whereas the fast or high-frequency inertia–gravity waves are filtered out. (When $V_T > 0$, the M mode could either be low frequency or high frequency, depending on the relative magnitude of V_T. For smaller V_T values, the M mode is a low-frequency mode, as described in the present section. For larger V_T values, on the other hand, the M mode is a high-frequency mode, and it is filtered out of the PQG system in the saturated phase; see section 6 below.)

d. Potential vorticity inversion

Given the two variables PV_e and M, all other variables can be obtained by solving a nonlinear elliptic PDE, as described next. Since both PV_e and M are needed as inputs, we will refer to this as PV-and-M inversion to distinguish it from the PV inversion of the dry QG system.

The PDE for PV-and-M inversion follows from the definition of PV_e in (26) by writing the right-hand side in terms of streamfunction ψ and also M:

$$\nabla_h^2\psi + \frac{f}{B_e}\frac{\partial}{\partial z}[H_u\theta_{eu}(\psi_z, M, z) + H_s\theta_{es}(\psi_z, M, z)] = \mathrm{PV}_e, \tag{32}$$

where $\zeta = \nabla_h^2\psi$ has been used, and θ_e has been written as a function of ψ_z and M in unsaturated and saturated regions. To write the functions $\theta_{eu}(\psi_z, M, z)$ and $\theta_{es}(\psi_z, M, z)$ in concrete form, relationships between θ_e, ψ_z, and M are needed. To this end, notice that the definition $M = q_t + G_M\theta_e$ can be used to rewrite (21) in terms of b_u, b_s, θ_e, and M as

$$b_u = g\left[\frac{\theta_e}{\theta_o} - \frac{L_v}{c_p\theta_o}(M - G_M\theta_e)\right] \quad \text{and} \tag{33a}$$

$$b_s = g\left[\frac{\theta_e}{\theta_o} - \frac{L_v}{c_p\theta_o}q_{vs}(z)\right]. \tag{33b}$$

Then, note that b_u and b_s can be replaced by $f\psi_z$ in unsaturated and saturated regions, respectively, since $f\psi_z = b_uH_u + b_sH_s$ from hydrostatic balance. Therefore, (33) can be used to write θ_e as

$$\theta_e = H_u\frac{1}{D_M}\left(\frac{f\theta_o}{g}\frac{\partial\psi}{\partial z} + \frac{L_v}{c_p}M\right) + H_s\left[\frac{f\theta_o}{g}\frac{\partial\psi}{\partial z} + \frac{L_v}{c_p}q_{vs}(z)\right], \tag{34}$$

where $D_M = 1 + L_vG_M/c_p$. This expression can then be used to write the PDE (32) in concrete form as

$$\nabla_h^2\psi + \frac{1}{D_M}\frac{f}{B_e}\frac{\partial}{\partial z}\left[H_u\left(\frac{f\theta_o}{g}\frac{\partial\psi}{\partial z} + \frac{L_v}{c_p}M\right)\right] + \frac{f}{B_e}\frac{\partial}{\partial z}\left\{H_s\left[\frac{f\theta_o}{g}\frac{\partial\psi}{\partial z} + \frac{L_v}{c_p}q_{vs}(z)\right]\right\} = \mathrm{PV}_e. \tag{35}$$

Finally, this PDE can be written in terms of the buoyancy frequencies, N_u^2 and N_s^2 from (25), as

$$\nabla_h^2\psi + \frac{\partial}{\partial z}\left[H_u\left(\frac{f^2}{N_u^2}\frac{\partial\psi}{\partial z} + \frac{L_v}{c_p}\frac{g}{\theta_0}\frac{f}{N_u^2}M\right)\right] + \frac{\partial}{\partial z}\left\{H_s\left[\frac{f^2}{N_s^2}\frac{\partial\psi}{\partial z} + \frac{L_v}{c_p}\frac{g}{\theta_0}\frac{f}{N_s^2}q_{vs}(z)\right]\right\} = \mathrm{PV}_e, \tag{36}$$

where the relations $N_u^2 = N_s^2[1 + (L_v/c_p)G_M] = N_s^2D_M$ and $N_s^2 = (g/\theta_0)B_e$ were used. This PDE defines a PV-and-M inversion for the PQG system.

Note that the unsaturated and saturated buoyancy frequencies, N_u and N_s, appear with the ψ_z terms of (36) in the familiar form of f^2/N^2, except here with different values in the different phases: f^2/N_u^2 in unsaturated regions and f^2/N_s^2 in saturated regions. In both phases, additional terms arise inside the vertical derivative in (36) because the potential vorticity variable PV_e is based on θ_e rather than one of the buoyancies b_u or b_s. In section 7 below, we compare this (θ_e, M) formulation to a formulation using (b_u, M).

Solving the PDE in (36) yields the streamfunction ψ, and then, all variables can be determined from ψ and M. For example, as in dry QG, the velocities u and v are recovered from geostrophic balance [(19a)], and θ is recovered from hydrostatic balance in (14), (19b), and (20). In addition, here in PQG, additional variables such as θ_e and q_t can be recovered. One can find θ_e from (34) and q_t from $q_t = M - G_M\theta_e$, where the choice of $H_u = 1$ or $H_s = 1$ in (34) is selected to be consistent with the resulting value of q_t.

Also notice that the phase interface is determined as part of the solution of the PV-and-M inversion process. As described in the previous paragraph, the value of q_t is known only after the streamfunction ψ has been found. Therefore, similarly, the location of the phase interface, and the values of the functions H_u and H_s, are outputs from, not inputs to, the PV-and-M inversion. This is illustrated concretely in the example solution in section 8. Because of the dependence of H_u and H_s on ψ, the elliptic PDE in (36) is nonlinear.

In summary, two variables, PV and M, are necessary and sufficient to determine the entire state of the PQG system, in contrast to the single variable PV for the dry QG system. Just as one must add an additional water variable (e.g., q_t) for moist thermodynamics to augment the dry state variables (e.g., p and θ), one must add one variable M for precipitating QG to augment the PV variable.

5. Energetics

The PQG equations conserve the following energy:

$$E = \frac{1}{2}\int_V\left\{|\nabla_h\psi|^2 + H_u\left(\frac{f^2}{N_u^2}\psi_z^2\right) + H_s\left(\frac{f^2}{N_s^2}\psi_z^2\right) + H_u\left[\left(\frac{L_v}{c_p}\frac{g}{\theta_0}\right)^2\frac{N_s^2}{N_u^2}\frac{1}{N_u^2 - N_s^2}\left(M - \frac{N_u^2}{N_s^2}q_{vs}\right)^2\right]\right\}dV, \tag{37}$$

where the domain V is assumed to be periodic in x and y, and the boundary conditions are $w = 0$ at upper and lower boundaries. It then follows from the PQG equations in section 3 that

$$\frac{dE}{dt} = 0. \tag{38}$$

The derivation is facilitated by many of the points of discussion in the following paragraphs and by noting that $(d/dt)\int_V G\,dV = \int_V (D_h G/Dt)\,dV$ for any function G because of the incompressibility of $\mathbf{u}_h$.

The energy in (37) involves the sum of four components: a kinetic energy KE involving $|\nabla_h \psi|^2$, an unsaturated potential energy PE_u involving $H_u \psi_z^2/N_u^2$, a saturated potential energy PE_s involving $H_s \psi_z^2/N_s^2$, and a moist energy ME involving M:

$$\mathrm{KE} = \frac{1}{2}\int_V |\nabla_h \psi|^2 dV, \tag{39}$$

$$\mathrm{PE}_u = \frac{1}{2}\int_V H_u \left(\frac{f^2}{N_u^2}\psi_z^2\right) dV, \tag{40}$$

$$\mathrm{PE}_s = \frac{1}{2}\int_V H_s \left(\frac{f^2}{N_s^2}\psi_z^2\right) dV, \quad \text{and} \tag{41}$$

$$\mathrm{ME} = \frac{1}{2}\int_V H_u \left[\left(\frac{L_v}{c_p}\frac{g}{\theta_0}\right)^2 \frac{N_s^2}{N_u^2}\frac{1}{N_u^2 - N_s^2}\left(M - \frac{N_u^2}{N_s^2} q_{vs}\right)^2\right] dV. \tag{42}$$

For comparison with the energy of the dry QG equations, notice the various contributions of water: 1) to the buoyancy frequency N_s^2 of the saturated potential energy, 2) to the determination of the form of the potential energy via the phase change, indicated by H_u and H_s, and 3) to the moist energy term ME, which involves $M = q_t + G_M \theta_e$.

Notice that the density of the total potential energy, $\mathrm{PE} = \mathrm{PE}_u + \mathrm{PE}_s + \mathrm{ME}$, is continuous across the phase interface even though each of the densities of the components PE_u, PE_s, and ME is, by itself, discontinuous across the phase interface. To see this, consider from ME the quantity $M - (N_u^2/N_s^2)q_{vs}$, which, in terms of q_t and θ_e, is $q_t + G_M\theta_e - (N_u^2/N_s^2)q_{vs}$. Notice that, at the phase interface, where $q_t = q_{vs}$, this quantity can be written as $(N_u^2 - N_s^2)N_s^{-2}(c_p/L_v)\theta = (N_u^2 - N_s^2)N_s^{-2}(c_p/L_v)(\theta_0/g)f\psi_z$. Hence, one can see that, at the phase interface, the integrand in the ME definition in (42) is equal to

$$H_u\left(\frac{f^2}{N_s^2} - \frac{f^2}{N_u^2}\right)\psi_z^2, \tag{43}$$

which ensures that the total potential energy density is continuous across the phase interface.

The energy transfers between the four components are

$$\frac{d}{dt}\mathrm{KE} = \int_V f w \psi_z\, dV, \tag{44}$$

$$\frac{d}{dt}\mathrm{PE}_u = -\int_V H_u f w \psi_z\, dV - \int_V \frac{f^2}{N_u^2}\psi_z^2 \frac{D_h H_s}{Dt} dV, \tag{45}$$

$$\frac{d}{dt}\mathrm{PE}_s = -\int_V H_s f w \psi_z\, dV + \int_V \frac{f^2}{N_s^2}\psi_z^2 \frac{D_h H_s}{Dt} dV, \quad \text{and} \tag{46}$$

$$\frac{d}{dt}\mathrm{ME} = \int_V \left(\frac{f^2}{N_u^2}\psi_z^2 - \frac{f^2}{N_s^2}\psi_z^2\right)\frac{D_h H_s}{Dt} dV. \tag{47}$$

These energy transfer equations follow from applying d/dt to each of the four definitions in (39)–(42). Also, to arrive at (47), the calculations leading to (43) were used.

Notice that the role of the moist energy ME is in the exchange of unsaturated PE_u and saturated potential energy PE_s, not in any direct energy transfer with kinetic energy. In fact, transfers of moist energy ME occur only at the location of the phase interface, as indicated by the $D_h H_s/Dt$ factor, which is proportional to a Dirac delta function δ that equals zero away from the phase interface. Explicitly, since $H_s(x, y, z, t) = \mathscr{H}[q_t(x, y, z, t) - q_{vs}(z)]$, where $\mathscr{H}$ is the Heaviside function, one can see that the $D_h H_s/Dt$ factor is equal to $\delta[q_t(x, y, z, t) - q_{vs}(z)]D_h q_t/Dt$. Hence, the integral over the volume V in (47) could be written as a surface integral over the phase interface. When the moist energy ME is transferred at the phase interface, it corresponds to a conversion between 1) latent potential energy that is not directly transferable to kinetic energy and 2) buoyant potential energy that is directly transferable to kinetic energy.

Alternative definitions of the M variable are suggested by the form of the moist energy ME in (42). Recall that the motivation for defining the variable $M = q_t + G_M\theta_e$ was in eliminating w from the PQG system (see section 4). To this end, the key property of M is that its equation of motion does not include a w term, unlike the equations of motion of, for example, θ_e and q_t. This key property, however, is not unique to the quantity $M = q_t + G_M\theta_e$; it is also satisfied by many alternative definitions of M. For instance, the quantity $\tilde{M} = M - N_u^2 N_s^{-2} q_{vs}(z)$ would also suffice, since $D_h\tilde{M}/Dt = D_h M/Dt$, and such a choice would simplify the expression for the moist energy ME in (42). Moreover, one could absorb additional factors such as $(g/\theta_0)(N_s/N_u)$ into the definition of M to further simplify (42). On the other hand, the present definition $M = q_t + G_M\theta_e$ is advantageous for its simple relationship with θ_e and q_t.

Finally, notice that an energy loss due to hydrometeor drag does not appear in the energy principle in (38). This is because the hydrometeor drag term $-gq_r$ in the buoyancy is asymptotically small in the PQG approximation applied here, as indicated by the asymptotic form [(20)] of the original buoyancy [(13)]. One could, alternatively, retain the hydrometeor drag term and hence also its dissipative effect on energy (Pauluis et al. 2000; Pauluis and Dias 2012; Hernandez-Duenas et al. 2013, 2015) as a small correction term that may be important on longer time scales; we plan to consider such effects elsewhere in the near future.

6. The limit of asymptotically large rainfall speed

For the rainfall speed V_T, a second scaling regime can be considered by assuming that V_T is relatively fast, in contrast to the scaling regime considered above in which V_T was comparable to the reference vertical velocity scale. For horizontal scale $L \sim 1000\,\mathrm{km}$, vertical scale $H \sim 10$ km, and characteristic horizontal velocity $U \sim 10\ \mathrm{m\,s^{-1}}$, the characteristic vertical velocity scale is $W \sim 0.1\ \mathrm{m\,s^{-1}}$. Thus, the scaled rainfall speed $V_r = V_T/W$ is relatively small for $V_T < 0.1\,\mathrm{m\,s^{-1}}$, relatively large for $V_T > 0.1\ \mathrm{m\,s^{-1}}$, and a rainfall speed $V_T \sim 1\,\mathrm{m\,s^{-1}}$ is asymptotically large. (As described in the appendix, the formal derivation of PQG uses an expansion in powers of ε, with a typical value of $\varepsilon \approx 0.1$ for standard reference quantities and thermodynamic parameters. Thus $V_T = 1\ \mathrm{m\,s^{-1}}$ corresponds to $V_r \approx 10 = \varepsilon^{-1}$.)

In the fast-V_T limit, the dominant balance in the q_t equation [(1d)] is

$$w\frac{d\tilde{q}_t}{dz} = V_T\frac{\partial q_r}{\partial z}, \quad \text{if saturated}, \tag{48}$$

where w and $\partial q_r/\partial z$ are small and $-d\tilde{q}_t/dz$ and V_T are large, such that the products in (48) are $O(1)$. In saturated regions, q_t dynamics are thus replaced by the constraint [(48)] relating small vertical velocity w to small vertical change in rain mixing ratio $\partial q_r/\partial z$. The PQG model is otherwise unaltered, and in particular, the PQG model is exactly the same in unsaturated flow regions for all values of V_T. Physically, (48) suggests that, within quasigeostrophic storms, the vertical velocity may be directly proportional to the change in rainfall mixing ratio with height. It would be interesting to investigate whether this balance is seen in observational data.

Some interesting remarks can be made regarding the balance [(48)]. Effectively, (48) is a closure for w in terms of q_r, which then gives the heating in terms of q_r by (23). Such a closure is reminiscent of convective parameterizations with heating proportional to water content (Lapeyre and Held 2004; Dias and Pauluis 2010; Lambaerts et al. 2012; Monteiro and Sukhatme 2016). However, note the important difference in the $V_T \to \infty$ PQG model: heating is proportional to the *change of rainfall mixing ratio with height*, as opposed to the rainfall mixing ratio itself. Furthermore, the PQG model describes large-scale dynamics, filtering out smaller-scale processes including convection, whereas convective adjustment models are meant to capture convection. As a final comment, (48) suggests that it may be feasible to find the vertical velocity through PV-and-M inversion alone, instead of by solving an omega equation (Sutcliffe 1947; Hoskins et al. 1978), but only in saturated flow regions. The physical implications of (48), its possible computational advantages, and the PQG omega equation will be explored elsewhere.

7. Alternate forms of potential vorticity

a. PV based on b_u

Alternate forms of the PQG model [(22)] result from replacing the equations for θ_e and q_t by the equations for any two linear combinations of θ_e and q_t. For a predominantly unsaturated background, a different sensible choice is to work with b_u and M. The equivalent PQG model combines the vorticity [(22a)] and the M equation [(29)] with (24b) for the unsaturated buoyancy b_u. The unsaturated buoyancy can be written in terms of ψ and M as

$$b_u = H_u f\frac{\partial\psi}{\partial z} + H_s\left[\frac{N_u^2}{N_s^2}\left(f\frac{\partial\psi}{\partial z} + \frac{L_v g}{c_p\theta_o}q_{vs}(z)\right) - \frac{L_v g}{c_p\theta_o}M\right], \tag{49}$$

where we have used the hydrostatic balance relation [(19b)], the asymptotic forms of the buoyancies [(21)], and the definition of M [(28)].

The unsaturated potential vorticity may be defined by

$$\mathrm{PV}_u = \nabla_h^2\psi + \frac{f}{N_u^2}\frac{\partial b_u}{\partial z} \tag{50}$$

in unsaturated and saturated regions. The evolution equation governing PV_u is given by

$$\frac{D_h \mathrm{PV}_u}{Dt} = -\frac{f}{N_u^2}\frac{\partial \mathbf{u}_h}{\partial z}\cdot\nabla_h b_u - V_T\frac{fL_v}{N_u^2 c_p}\frac{\partial^2 q_r}{\partial z^2}, \tag{51}$$

and must be coupled to the M equation [(29)]. Note the appearance of a rainfall term on the right-hand side of the PV_u equation [(51)], which does not appear in the PV_e formulation. Finally, PV_u-and-M inversion follows from (49) and (50):

$$\nabla_h^2\psi + \frac{\partial}{\partial z}\left[H_u\frac{f^2}{N_u^2}\frac{\partial\psi}{\partial z} + H_s\left(\frac{f^2}{N_s^2}\frac{\partial\psi}{\partial z} + \frac{f}{N_s^2}\frac{L_v g}{c_p\theta_0}q_{vs} - \frac{f}{N_u^2}\frac{L_v g}{c_p\theta_0}M\right)\right] = \mathrm{PV}_u. \qquad (52)$$

b. PV based on b or virtual potential temperature

As another choice, one could define PV based on the virtual potential temperature θ_v^{tot}. Several advantageous features of this choice have been discussed by Schubert et al. (2001) in a more comprehensive model of moist dynamics that does not assume quasigeostrophic scaling. In the PQG model, anomalies of virtual potential temperature are proportional to the buoyancy variable b, and a corresponding PV variable could be defined as

$$\mathrm{PV}_v = \zeta + \frac{f}{N_u^2}\frac{\partial b}{\partial z} \qquad (53a)$$

$$= \zeta + \frac{f}{N_u^2}\frac{\partial}{\partial z}(H_u b_u + H_s b_s). \qquad (53b)$$

Because of phase changes, this definition involves several subtleties.

First, notice that PV_v is *discontinuous by definition*. This is because its definition in (53b) involves a $\partial/\partial z$ derivative of different quantities (b_u and b_s) in different phases, a consequence of the piecewise equation of state of the buoyancy: $b = H_u b_u + H_s b_s$. With discontinuous jumps at the phase interface, PV_v is somewhat similar to vortex patches of incompressible flow (Majda and Bertozzi 2002), which involve discontinuous jumps in vorticity over different spatial regions.

Second, notice that PV_v inversion is possible without the need for M. Since $b = f\psi_z$, the definition [(53)] can be used to define an elliptic PDE for PV_v inversion:

$$\nabla_h^2\psi + \frac{f^2}{N_u^2}\frac{\partial^2\psi}{\partial z^2} = \mathrm{PV}_v. \qquad (54)$$

One subtlety here is that PV_v is discontinuous at the phase interface; consequently, the second derivatives such as ψ_{zz} are also discontinuous at the phase interface, and numerical methods must be designed carefully with these issues in mind. Aside from this subtlety, the form of this PV_v inversion appears superficially to be the same as in dry PV inversion. Given PV_v alone, this equation can be solved for ψ, from which one can compute the velocity $\mathbf{u}_h$ and buoyancy b. Then, as a subsequent step, one can use M or possibly some other variable such as q_t to determine all other variables. In contrast to PV-and-M inversion, the location of the phase interface is already known a priori from the locations of the discontinuous jumps in PV_v.

Third, the evolution equation for PV_v has some differences compared to that of PV_e or PV_u, due in part to the discontinuous definition of PV_v. If the operator D_h/Dt is applied to the definition in (53b), the result is

$$\frac{D_h\mathrm{PV}_v}{Dt} = \frac{f}{N_u^2}\frac{\partial}{\partial z}\left(-\frac{d\tilde{q}_{vs}}{dz}wH_s\right) \qquad (55a)$$

$$= -\frac{f}{N_u^2}\frac{d\tilde{q}_{vs}}{dz}\frac{\partial w}{\partial z}H_s - \frac{f}{N_u^2}\frac{d\tilde{q}_{vs}}{dz}w\frac{\partial H_s}{\partial z}, \qquad (55b)$$

which has some potential advantages and disadvantages. One advantageous feature in (55a) is that the dynamics are a conservation law with a perfect derivative on the right-hand side. On the other hand, several complex features are also apparent. For instance, vertical velocity w is not completely eliminated from the dynamics; its appearance represents a heat source term. (For the case of large V_T, however, one may be able to still eliminate w by taking advantage of the relationship between w and $\partial q_r/\partial z$; see section 6 above.) In addition, the factor $\partial H_s/\partial z$ is a Dirac delta function that is supported on the phase interface. For comparison, these features would be represented by the term involving $\nabla\dot{\theta}_\rho$ in (20) and (21) of Schubert et al. (2001). Because of these features, it is possible that the use of PV_v as a dynamical variable may be complicated despite its potential use as a diagnostic variable for PV_v inversion. It would be interesting to investigate the advantages and disadvantages of the many different PV definitions in more detail in the future.

8. Example PV-and-M inversion and determination of phase boundary

In this section, an example of PV-and-M inversion is presented to illustrate the new effects of phase changes, for comparison with traditional PV inversion. In particular, here, the two variables PV_u and M are given, and the locations of phase boundaries are not known a priori; the phase boundaries and all other variables (streamfunction ψ, potential temperature θ, total water q_t, etc.) are determined from the solution of the PV-and-M inversion problem.

a. Setup

For this simple example, the PV_u formulation [(52)] is discretized using centered differences in the vertical direction following similar discretizations for dry QG equations (e.g., Phillips 1954). See Fig. 1. In the case of two vertical levels, the dynamical variables are ψ_1 for the lower troposphere and ψ_2 for the upper

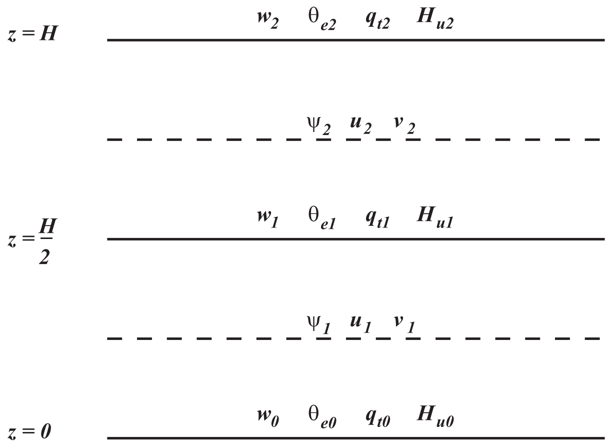

FIG. 1. Variables in the two-level system.

troposphere. For convenience, one can use vertical modes instead of vertical levels, where the barotropic mode is $\psi = (\psi_1 + \psi_2)/2$ and the baroclinic mode is $\tau = (\psi_2 - \psi_1)/2$. One can show that the PV inversion for the baroclinic mode is

$$\nabla_h^2\tau - 8(H_uF_u^2 + H_sF_s^2)\tau = \mathrm{PV}_u - H_s\left(2F_uM - 2F_u\frac{F_s^2}{F_u^2}q_{vs}\right), \tag{56}$$

where the subscript "1" has been dropped from several variables to ease notation, and variables at the upper and lower boundaries have been set to zero for a simple choice of boundary conditions. Nondimensional units are used here, as described in the appendix, with $F_u = L/L_{du}$ and $F_s = L/L_{ds}$. Note that H_u and H_s are functions of τ, so this PDE is nonlinear.

As a simple case for illustration, consider an idealization of a cold-core cyclone by choosing a point-potential-vorticity distribution of

$$\mathrm{PV}_u(r) = \Gamma_\tau\delta(r), \tag{57}$$

where $r = (x^2 + y^2)^{1/2}$ is the distance from the origin and $\delta(r)$ is the Dirac delta function. Furthermore, choose the other parameters to also be axisymmetric: $M = M(r)$ and $q_{vs} = q_{vs}(r)$. Then seek solutions that are axisymmetric, in which case, in cylindrical polar coordinates, the equation satisfied by τ is

$$\frac{1}{r}\left[\frac{\partial}{\partial r}\left(r\frac{\partial\tau}{\partial r}\right)\right] - 8(H_uF_u^2 + H_sF_s^2)\tau = \Gamma_\tau\delta(r) - H_s\left(2F_uM - 2F_u\frac{F_s^2}{F_u^2}q_{vs}\right), \tag{58}$$

where the solution is assumed to tend toward the unsaturated background state (i.e., $\tau \to 0$) as $r \to \infty$. The specific values of the parameters used here are $\Gamma_\tau = 1.0$, $M = 0$, $q_{vs} = 0.1$, $F_u = 1.0$, and $F_s = \sqrt{2}$. These values were selected as simple nondimensional numerical values, and it will be shown below that they lead to a solution with somewhat reasonable physical values as well.

b. *Method for finding a solution*

To find a solution to (58), consider the following initial guess (and look forward to Figs. 2 and 3 for illustrations of the final result). As an initial guess, we suppose that the solution is saturated near the center of the vortex at $r = 0$. This is consistent with (58) and the choices $\Gamma_\tau > 0$ and $M = 0$, as can be seen by solving (58) under the assumption of saturated conditions [see (59) and Fig. 2 below]. However, the total water q_t should decrease away from the vortex center and eventually fall below the saturation value q_{vs}. Furthermore, the condition $\tau \to 0$ as $r \to \infty$ implies the anomaly $q_t \to 0$ as $r \to \infty$, and hence, the solution tends toward the unsaturated background state as $r \to \infty$. Combining these pieces, one can guess that the solution may consist of a saturated interior region near the vortex center and an unsaturated exterior region away from the vortex center, with a phase interface at some location $r = r_i$.

Note that this initial guess may not be correct; that is, it is possible, for instance, that the solution is saturated in regions $0 < r < r_1$ and $r_2 < r < r_3$ and unsaturated in regions $r_1 < r < r_2$ and $r > r_3$. The locations and numbers of saturated and unsaturated regions are not known a priori; they will be discovered as part of the process of solving the nonlinear elliptic PDE in (58). Nevertheless, one can imagine an iterative solution method for (58) in which one makes a first guess and then continues to update the guess until the iterations have converged. We are currently developing such a numerical method and will present it elsewhere in the near future. For now, for the example considered here, it is shown below that the first guess actually provides a solution, which has a single phase interface at $r = r_i$.

Continuing in a more precise way, a solution to (58) can be found using the intuition from the previous paragraphs and using the method of undetermined coefficients. First, suppose the solution is saturated ($H_u = 0$, $H_s = 1$) for $r < r_i$, where r_i is an unknown interface location. In this region, the solution has the form

$$\tau_s(r) = -\frac{\Gamma_\tau}{2\pi}K_0(k_sr) + BI_0(k_sr) - \frac{q_{vs}}{4F_u}, \tag{59}$$

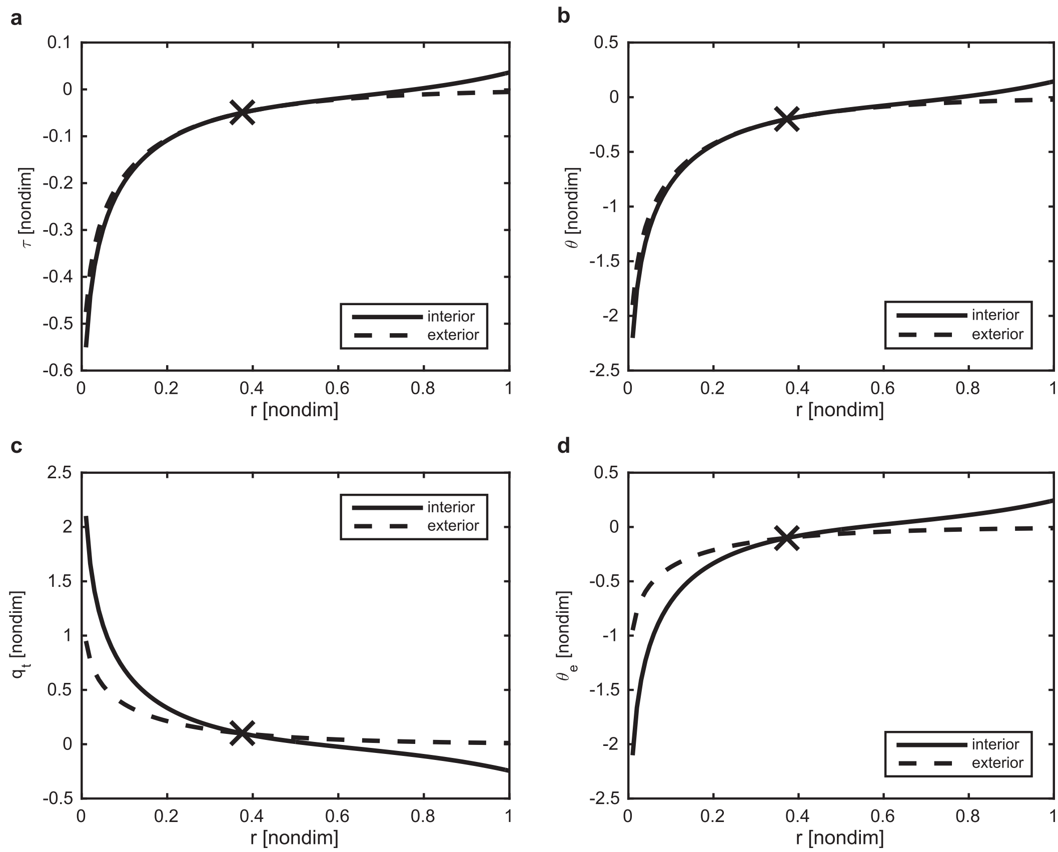

FIG. 2. Semianalytic solution of a PV-and-M inversion problem. Variables plotted are (a) baroclinic streamfunction τ, (b) potential temperature θ, (c) total water q_t, and (d) equivalent potential temperature θ_e, all as functions of r, the distance from the vortex center. The saturated interior solution is denoted by solid black curve, and unsaturated exterior solution is denoted by dashed black curve. The black cross indicates the phase interface, $r = r_i = 0.3743$. The functional form of the solution is shown in (59) and (60), and the PV-and-M inversion PDE is shown in (58).

where $k_s^2 = 8F_s^2$, and $K_0(r)$ and $I_0(r)$ are modified Bessel functions of the first and second kinds, respectively. The coefficient B is to be determined via the interface conditions. Second, suppose the solution is unsaturated ($H_u = 1$, $H_s = 0$) for $r > r_i$. Then the solution within this region has the form

$$\tau_u(r) = AK_0(k_u r), \tag{60}$$

where $k_u^2 = 8F_u^2$, and the coefficient A is to be determined via the interface conditions. Third, the interface conditions are:

$$q_t(r_i) = q_{vs}, \tag{61}$$

$$\tau_s(r_i) = \tau_u(r_i), \quad \text{and} \tag{62}$$

$$\tau_s'(r_i) = \tau_u'(r_i). \tag{63}$$

The first two [(61) and (62)] represent the saturation condition and continuity-of-pressure condition, respectively. The third [(63)] is the "jump condition" (Evans 1998; LeVeque 2002) that describes the jump in the value of $\partial\tau/\partial r$ at the interface; the jump turns out to be zero in this case. This third condition [(63)] arises from multiplying (58) by r, integrating from $r_i - \varepsilon$ to $r_i + \varepsilon$, and taking the limit $\varepsilon \to 0$. Physically, (63) indicates that the azimuthal velocity is continuous, since the azimuthal velocity equals $\partial\tau/\partial r$. Finally, note that (61)–(63) is a system of three nonlinear algebraic equations that can be solved to determine the unknown parameters A, B, and r_i, which in turn determine the solution $\tau(r)$.

c. Solution and illustration

We solved the system [(61)–(63)] numerically using an iterative algorithm with the command "fsolve" of the MATLAB computer software package. The solution is $A = -0.1291$, $B = 0.0056$, and $r_i = 0.3743$, in nondimensional units.

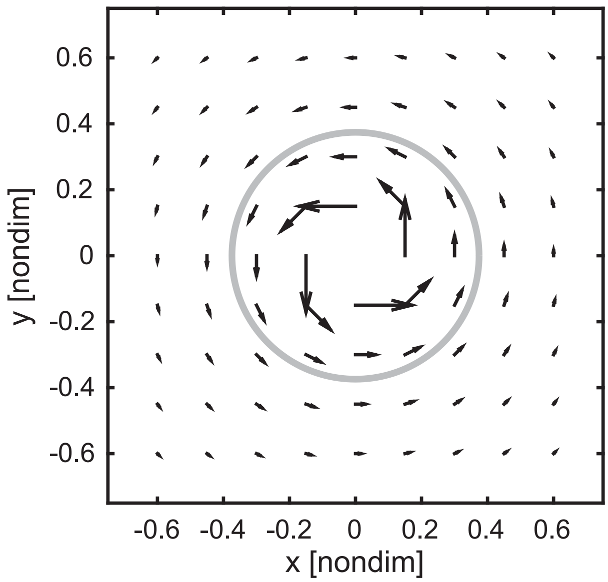

FIG. 3. Vector field $u(x, y)$, $v(x, y)$ in the upper troposphere for the semianalytic solution of the PV-and-M inversion problem. The gray circle indicates the radius $r = r_i = 0.3743$ of the phase interface that separates the saturated interior from the unsaturated exterior. See Fig. 2 for corresponding plots of other variables, and see (59) and (60) for the functional form of the solution and (58) for the PV-and-M inversion PDE.

The solution is illustrated in Figs. 2 and 3. The solution is saturated ($q_t > q_{vs}$) in the interior region ($r < r_i$) of the vortex, unsaturated ($q_t < q_{vs}$) in the exterior region ($r > r_i$) of the vortex, and tending toward the environmental state ($q_t \to 0$ as $r \to \infty$). Note the subtle discontinuities in this solution: each of the variables τ, θ, q_t, and θ_e is continuous, but the derivatives dq_t/dr and $d\theta_e/dr$ have jumps at the phase interface. Such discontinuities can present challenges for designing numerical methods for PV-and-M inversion with high-order accuracy, which we are currently pursuing.

In summary, in PQG, all variables can be recovered, through an inversion process, from knowledge of PV_u and M alone. Differences from dry PV inversion include 1) the need for a second variable M in addition to PV, 2) nonlinearity in the elliptic PDE for PV-and-M inversion, because of phase changes, and 3) the determination of unknown phase interface locations via the inversion process.

9. Generalized cloud microphysics, more comprehensive thermodynamics, and anelastic version of PQG equations

A primary reason to start with the minimal FARE model was to clearly and concretely illustrate the main features of the PQG model and the PV-and-M inversion with phase changes. Recall that ingredients of the FARE mode are Boussinesq dynamics, linearized thermodynamics, and asymptotically fast cloud microphysics. However, it is feasible to extend the analysis to include anelastic effects, and/or more comprehensive thermodynamics, and/or generalized cloud microphysics; these are the topics of the present section. These extensions show that PQG equations are not limited to idealized microphysics; PQG equations can in fact be derived for more comprehensive dynamics of a moist atmosphere and, as such, should represent the limiting dynamics of a moist atmosphere in the limit of rapid rotation and strong stratification.

a. An anelastic FARE model

The anelastic version of the FARE model is given by

$$\frac{D\mathbf{u}}{Dt} + f\hat{\mathbf{z}} \times \mathbf{u} = -\nabla\left[\frac{p}{\tilde{\rho}(z)}\right] + \hat{\mathbf{z}}\,b, \quad \text{(64a)}$$

$$\nabla \cdot [\tilde{\rho}(z)\mathbf{u}] = 0, \quad \text{(64b)}$$

$$\frac{D\theta_e}{Dt} + w\frac{d\tilde{\theta}_e}{dz} = 0, \quad \text{and} \quad \text{(64c)}$$

$$\frac{Dq_t}{Dt} + w\frac{d\tilde{q}_t}{dz} - \frac{1}{\tilde{\rho}}\frac{\partial}{\partial z}(\tilde{\rho}V_T q_r) = 0, \quad \text{(64d)}$$

where $\tilde{\rho}(z)$ is the background density profile. Then a derivation similar to that in section 3 or the appendix leads to the anelastic version of the PQG equations, which includes the balance relations

$$f\hat{\mathbf{z}} \times \mathbf{u}_h = -\nabla_h\phi, \quad b_u H_u + b_s H_s = \frac{\partial\phi}{\partial z}, \quad \text{(65)}$$

where $\phi = p/\tilde{\rho}(z)$, and $\psi = \phi/f$, and the dynamic equations

$$\frac{D_h\zeta}{Dt} = \frac{f}{\tilde{\rho}}\frac{\partial}{\partial z}(\tilde{\rho}w), \quad \text{(66a)}$$

$$\frac{D_h\theta_e}{Dt} + w\frac{d\tilde{\theta}_e}{dz} = 0, \quad \text{and} \quad \text{(66b)}$$

$$\frac{D_h q_t}{Dt} + w\frac{d\tilde{q}_t}{dz} - \frac{1}{\tilde{\rho}}\frac{\partial}{\partial z}(\tilde{\rho}V_T q_r) = 0. \quad \text{(66c)}$$

At this stage, the main difference from the Boussinesq case is in the appearance of the background density profile $\tilde{\rho}(z)$.

As a next step, as in sections 4 and 7 above, it is convenient to eliminate w and formulate the PQG system in terms of PV and the variable M. For the anelastic system, the definitions are

$$\mathrm{PV}_e = \zeta + \frac{f}{\tilde{\rho}}\frac{\partial}{\partial z}\left(\frac{\tilde{\rho}}{d\tilde{\theta}_e/dz}\theta_e\right) \quad \text{and} \tag{67}$$

$$M = q_t + G_M\theta_e, \tag{68}$$

where $G_M = -(d\tilde{q}_t/dz)/(d\tilde{\theta}_e/dz)$. Again, the main difference from the Boussinesq case is in the appearance of the background density profile $\tilde{\rho}(z)$; here, it is in the definition of PV_e. The definition of M is the same in the Boussinesq and anelastic cases.

b. A choice of thermodynamics

To formulate the PV-and-M inversion problem, a choice of thermodynamics is required. Specifically, one must write θ_e as a function of ψ_z and M in order to turn (67) into an elliptic PDE for streamfunction ψ. To do this, one should specify the relationships among all of the thermodynamic variables, such as θ_e, q_t, θ, q_v, buoyancy b, or virtual equivalent potential temperature θ_v. Several options are possible. One option is to use a linearized form of thermodynamics, as in the FARE model of section 2, with

$$\theta_e^{\mathrm{tot}} = \theta^{\mathrm{tot}} + \frac{L_v\tilde{\theta}(z)}{c_p\tilde{T}(z)}q_v^{\mathrm{tot}}, \tag{69}$$

etc. A second option would be to retain a more comprehensive and/or standard definition of thermodynamics, including, for instance

$$\theta_e^{\mathrm{tot}} = \theta^{\mathrm{tot}}\exp\left(\frac{L_v q_v^{\mathrm{tot}}}{c_p T^{\mathrm{tot}}}\right). \tag{70}$$

Similarly, the saturation profile could more realistically be allowed to vary with temperature, rather than depending only on altitude. Relation (70) is a *nonlinear* relationship between thermodynamic variables, and it results in a PV-and-M inversion that can be written abstractly as

$$\nabla_h^2\psi + \frac{f}{\tilde{\rho}}\frac{\partial}{\partial z}\left\{\frac{\tilde{\rho}}{d\tilde{\theta}_e/dz}[H_u\theta_{eu}(\psi_z, M, z) + H_s\theta_{es}(\psi_z, M, z)]\right\} = \mathrm{PV}_e, \tag{71}$$

where $\theta_{eu}(\psi_z, M, z)$ and $\theta_{es}(\psi_z, M, z)$ are the functions that define θ_e in terms of ψ_z and M in unsaturated and saturated regions, respectively. Although (71) is conceptually straightforward, the functions θ_{eu} and θ_{es} are complicated if not impossible to write down analytically in closed form because of the complicated nonlinearity in (70).

c. More comprehensive cloud microphysics

One could also use more comprehensive cloud microphysics by relaxing the assumptions of fast autoconversion and evaporation and by including more variables such as cloud ice q_i and number density and n_c of cloud droplets (e.g., Kessler 1969; Lin et al. 1983; Seifert and Beheng 2001, 2006). Then, the PQG model would consist of more equations in addition to those for θ_e and q_t.

To illustrate, consider warm-rain bulk cloud microphysics with finite time scales for condensation, evaporation, autoconversion, and collection but neglecting supersaturation. In this case, the starting point is (64) together with an equation for the mixing ratio of rainwater q_r:

$$\frac{Dq_r}{Dt} - \frac{1}{\tilde{\rho}}\frac{\partial}{\partial z}(\tilde{\rho}V_T q_r) = A_r + C_r - E_r, \tag{72}$$

where A_r, C_r, and E_r represent, respectively, autoconversion of cloud water to form rainwater, collection of cloud water to form rainwater, and evaporation of rainwater to form water vapor. Then, through a derivation similar to that in section 3 or the appendix, one arrives at a quasigeostrophic system including (65) and (66) together with the quasigeostrophic version of the dynamics [(72)] of rainwater:

$$\frac{D_h q_r}{Dt} - \frac{1}{\tilde{\rho}}\frac{\partial}{\partial z}(\tilde{\rho}V_T q_r) = A_r + C_r - E_r. \tag{73}$$

Notice that the only change from (72) to its quasigeostrophic version [(73)] is in the loss of the vertical advection term $w\partial q_r/\partial z$. Also notice that there is no term for vertical advection of background rainwater, since the background rainwater $\tilde{q}_r(z)$ is zero.

This evolution equation for q_r supplements the evolution equations of PV_e and M. Also, the PV-and-M inversion [(71)] is modified to become PV-and-M-and-q_r inversion, where all variables can be recovered from knowledge of the three variables PV, M, and q_r. Of course, closures for the source terms A_r, C_r, and E_r and/or assumptions about their asymptotic quasigeostrophic scaling are now also required. Thus, additional hydrometeors require additional evolution equations and introduce complexity through source terms, but the fundamental ideas of the PQG structure are similar for any choice of cloud microphysics.

10. Discussion and conclusions

In summary, precipitating quasigeostrophic equations were derived systematically. The PQG system includes the nonlinear effects of phase changes, which arise, for instance, through separate buoyancy frequencies N_u and N_s for unsaturated and saturated regions, respectively. An energy principle was also presented, and the potential energy was shown to change across phase boundaries and to include the effects of a moist energy.

Two variables, a potential vorticity and a moist variable M, were shown to be necessary and sufficient to characterize the simplest version of the PQG system. Given these two variables, all other variables can be found as outputs from a PV-and-M inversion process. The PDE for PV-and-M inversion is elliptic and nonlinear, because of the effects of phase changes. In PV-and-M inversion, the location of the phase interface is unknown a priori and is discovered as an output of the inversion process.

Cases with more general cloud microphysics were also considered. From a theoretical point of view, these cases show that the PQG equations are not limited to idealized microphysics; PQG equations can in fact be derived for more comprehensive dynamics of a moist atmosphere, and they therefore represent the limiting dynamics of a moist atmosphere, in the limit of rapid rotation and strong (moist) stratification. From a more practical point of view, in cases with more general microphysics, additional variables are needed beyond a potential vorticity and the moist variable M. For example, the case of Kessler (1969) warm-rain microphysics was described in section 9. In this case, a rainwater mixing ratio q_r is also needed. For other cases involving ice and/or double-moment microphysics, additional variables are needed. Nevertheless, the basic principles of the PQG system and its derivation are similar to the case of idealized microphysics.

Finally, we end with three directions, in addition to the linear analysis of meridional moisture transport (Wetzel et al. 2017, manuscript submitted to *Math. Climate Wea. Forecasting*), that will be interesting to pursue in the future.

First, numerical simulations of the PQG system can provide a simplified setting, compared to global climate model simulations, for investigating the hydrological cycle and effects of latent heat release. For example, the PQG model could potentially provide insight into the appropriate effective static stability for a moist atmosphere (e.g., Lapeyre and Held 2004; O'Gorman 2011). We are currently designing numerical methods for the PV-and-M inversion problem, which are needed for simulating the dynamics of the PQG system, and results will be presented elsewhere in the future.

Second, for simplicity in this first investigation with phase changes, all condensational heating was assumed to be associated with quasigeostrophic motions, and the effects of smaller-scale convection were neglected. It would be interesting to include mesoscale convective effects and their impacts on the synoptic-scale QG dynamics in the future.

Third, precipitation introduces a potential dissipation mechanism that is not present in dry dynamics (Pauluis et al. 2000; Pauluis and Dias 2012; Hernandez-Duenas et al. 2013). In the present paper, though, the dissipative effects of precipitation were not present in the leading-order dynamics, as the leading-order buoyancy [(20)] was simply $g\theta/\theta_0$ and did not include the hydrometeor drag term $-gq_r$ from (13). Nevertheless, it would be interesting to retain the hydrometeor drag term in future studies, along with other dissipation mechanisms such as frictional drag and radiative cooling, to investigate the relative roles of different dissipation mechanisms in a precipitating setting.

Acknowledgments. The research of L.M.S. and S.N.S. is partially supported by Grant NSF AGS 1443325. The research of S.N.S. is also partially supported by a Sloan Research Fellowship. The authors are grateful for valuable input from Juliana Dias, Thomas Edwards, Gerardo Hernandez-Duenas, Jonathan Martin, Olivier Pauluis, Grant Petty, Chung-Nan Tzou, Geoff Vallis, Fabian Waleffe, Alfredo Wetzel, and two anonymous reviewers.

APPENDIX

Systematic Asymptotic Derivation of the PQG Equations

a. The nondimensionalized FARE equations

Using the reference scales defined in Table A1, the FARE model [(1)] may be rewritten in nondimensional form as

$$\frac{D_h\mathbf{u}_h}{Dt} + w\frac{\partial \mathbf{u}_h}{\partial z} + \mathrm{Ro}^{-1}\mathbf{u}_h^{\perp} + \mathrm{Eu}\nabla_h p = 0, \tag{A1a}$$

$$A^2\left(\frac{D_h w}{Dt} + w\frac{\partial w}{\partial z}\right) + \mathrm{Eu}\frac{\partial p}{\partial z} - \Gamma A^2(b_u H_u + b_s H_s) = 0, \tag{A1b}$$

$$\nabla_h \cdot \mathbf{u}_h + \frac{\partial w}{\partial z} = 0, \tag{A1c}$$

$$\frac{D_h b_u}{Dt} + w\frac{\partial b_u}{\partial z} + \mathrm{Fr}_u^{-2}(\Gamma A^2)^{-1}w + V_r\left(1 - R_{vd}\frac{c_p\theta_o}{L_v}\right)\frac{\partial q_r}{\partial z} = 0, \quad \text{and} \tag{A1d}$$

$$\frac{D_h b_s}{Dt} + w\frac{\partial b_s}{\partial z} + \mathrm{Fr}_s^{-2}(\Gamma A^2)^{-1}w + V_r\frac{c_p\theta_o}{L_v}\frac{\partial q_r}{\partial z} = 0, \tag{A1e}$$

TABLE A1. Reference scales used for the nondimensionalization.

Variable	Reference scale
x, y	L
z	H
t	$\tau = L/U$
$u(\mathbf{x}, t)$, $v(\mathbf{x}, t)$	U
$w(\mathbf{x}, t)$	$W = UH/L$
$p(\mathbf{x}, t)$	$\overline{P}$
$\theta(\mathbf{x}, t)$, $\theta_e(\mathbf{x}, t)$	Θ
$q_v(\mathbf{x}, t)$, $q_r(\mathbf{x}, t)$, $q_t(\mathbf{x}, t)$, $q_{vs}(z)$, $M(\mathbf{x}, t)$	$Q = c_p\Theta/L_v$
$b_u(\mathbf{x}, t)$, $b_s(\mathbf{x}, t)$, $b(\mathbf{x}, t)$	$B = g\Theta/\theta_o$

TABLE A2. Dimensionless quantities from the FARE model.

Symbol	Definition	Name (notes)
Ro	$U(Lf)^{-1}$	Rossby number
Eu	$\overline{P}(\rho_o U^2)^{-1}$	Euler number
Fr_u	$U(N_u H)^{-1}$	Froude number (unsaturated)
Fr_s	$U(N_s H)^{-1}$	Froude number (saturated)
Γ	$BHW^{-2} = g\Theta\theta_o^{-1}L^2(U^2H)^{-1}$	(buoyancy parameter)
A	HL^{-1}	Aspect ratio
V_r	$V_T W^{-1} = V_T L(HU)^{-1}$	Rainfall speed

where $\mathbf{u}_h^\perp = (-v, u)$, and we have combined the equations for (θ_e, q_t) into equations for (b_u, b_s) using the definitions [(17)]. The nondimensional numbers are defined in Table A2: the Rossby number Ro, Euler number Eu, Froude numbers Fr_u and Fr_s, aspect ratio A, fall speed V_r, and buoyancy parameter Γ. The buoyancy anomalies [(17)] may be written in nondimensional form as

$$b_u = \left[\theta_e + \left(R_{vd}\frac{c_p\theta_o}{L_v} - 1\right)q_t\right] \quad \text{and} \tag{A2a}$$

$$b_s = \left[\theta_e + \left(R_{vd}\frac{c_p\theta_o}{L_v} - 1 + \frac{c_p\theta_o}{L_v}\right)q_{vs}(z) - \frac{c_p\theta_o}{L_v}q_t\right]. \tag{A2b}$$

The Rossby deformation scales are

$$L_{du} = \frac{N_u H}{f}, \quad L_{ds} = \frac{N_s H}{f}, \tag{A3}$$

where H is the height of the troposphere. The unsaturated and saturated buoyancy frequencies N_u, N_s are given by

$$N_u^2 = g\frac{d}{dz}\left[\frac{\tilde{\theta}_e}{\theta_o} + \left(R_{vd} - \frac{L_v}{c_p\theta_o}\right)\tilde{q}_t\right] \quad \text{and} \tag{A4a}$$

$$N_s^2 = g\frac{d}{dz}\left[\frac{\tilde{\theta}_e}{\theta_o} - \left(R_{vd} - \frac{L_v}{c_p\theta_o} + 1\right)q_{vs}(z) - \tilde{q}_t\right]. \tag{A4b}$$

Note that N_u^2 could be thought of as the vertical derivative of a background buoyancy $\tilde{b}_u$, but this type of interpretation is less simple for N_s^2. To arrive at the definition of N_s^2, a material derivative D/Dt is applied to the definition of b_s in (A2b), and the resulting background terms are grouped together into the definition of N_s^2; the term $[R_{vd} - L_v(c_p\theta_o)^{-1} + 1]q_{vs}(z)$ has a sign change in comparing b_s in (A2b) and N_s^2 in (A4), which complicates the interpretation of N_s^2 as the vertical derivative of a background buoyancy $\tilde{b}_s$. In fact, the variables b_u and b_s were *defined* in terms of the *anomalous* variables θ_e and q_t in (17) without defining any corresponding background states for b_u and b_s.

b. *Derivation of the PQG equations*

Similar to the dry case, we consider horizontal length scale $L \sim L_{du} \sim L_{ds}$, and we assume a rapidly rotating and strongly stably stratified flow with asymptotic scalings:

$$\mathrm{Ro} = \mathrm{Eu}^{-1} = \varepsilon, \quad \mathrm{Fr}_u = \frac{L}{L_{du}}\mathrm{Ro} = O(\varepsilon),$$
$$\mathrm{Fr}_s = \frac{L}{L_{ds}}\mathrm{Ro} = O(\varepsilon), \quad \Gamma A^2 = \mathrm{Fr}_u^{-1}, \tag{A5}$$

which look like the same assumption as in the derivation of dry QG except that background water profiles are hidden in the two Froude numbers Fr_u and Fr_s and we have two Froude numbers instead of one. (Note that either $\mathrm{Ro} = \varepsilon$ or $\mathrm{Eu}^{-1} = \varepsilon$ could be taken as the definition of ε, since Ro and Eu^{-1} are taken to be equal to each other.) Introducing characteristic scales denoted Θ and $Q = c_p\Theta/L_v$, respectively, for the anomalies of potential temperature and water mixing ratios, it follows from $\mathrm{Fr}_u \sim \mathrm{Fr}_s = O(\varepsilon)$ that

$$\tilde{G}_M = -\frac{\Theta}{Q}\frac{d\tilde{q}_t/dz}{d\tilde{\theta}_e/dz} = -\frac{L_v}{c_p}\frac{d\tilde{q}_t/dz}{d\tilde{\theta}_e/dz} = O(1), \tag{A6}$$

which is a nondimensional version of the parameter G_M of the main text. Additional assumptions are

$$\frac{gQ}{B} = \frac{c_p\theta_o}{L_v} = C_{cl}\mathrm{Ro} = O(\varepsilon), \quad V_r = O(1), \tag{A7}$$

where C_{cl} is an $O(1)$ constant. The first relation in (A7) says that the ratio of buoyancy anomalies gQ/B is small, where $B = g\Theta/\theta_o$. On the other hand, from (A6), we consider the normalized background slopes $Q^{-1}d\tilde{q}_t/dz$ and $\Theta^{-1}d\tilde{\theta}_e/dz$ to be the same order of magnitude.

The distinguished limit [(A5)–(A7)] leads to the equations

$$\frac{D_h\mathbf{u}_h}{Dt} + w\frac{\partial \mathbf{u}_h}{\partial z} + \varepsilon^{-1}\mathbf{u}_h^{\perp} + \varepsilon^{-1}\nabla_h p = 0 \qquad \text{(A8a)}$$

$$A^2\left(\frac{D_h w}{Dt} + w\frac{\partial w}{\partial z}\right) + \varepsilon^{-1}\frac{\partial p}{\partial z} - \varepsilon^{-1}\frac{L_{du}}{L}(b_u H_u + b_s H_s) = 0, \qquad \text{(A8b)}$$

$$\nabla_h \cdot \mathbf{u}_h + \frac{\partial w}{\partial z} = 0, \qquad \text{(A8c)}$$

$$\frac{D_h b_u}{Dt} + w\frac{\partial b_u}{\partial z} + \varepsilon^{-1}\frac{L_{du}}{L}w + V_r(1 - R_{vd}\varepsilon C_{cl})\frac{\partial q_r}{\partial z} = 0, \quad \text{and} \qquad \text{(A8d)}$$

$$\frac{D_h b_s}{Dt} + w\frac{\partial b_s}{\partial z} + \varepsilon^{-1}\frac{L_{ds}}{L}w + \varepsilon V_r C_{cl}\frac{\partial q_r}{\partial z} = 0. \qquad \text{(A8e)}$$

With the values $\theta_o \approx 300\,\mathrm{K}$, $L_v \approx 2.5\times10^6\,\mathrm{J\,kg^{-1}}$, and $c_p \approx 10^3\,\mathrm{J\,kg^{-1}\,K^{-1}}$, a typical value of ε would then be $\varepsilon \approx 0.12$. The assumed scaling is consistent with potential temperature anomaly scale $\Theta \approx 3\,\mathrm{K}$ and midlatitude horizontal velocity scale $U \approx 10\,\mathrm{m\,s^{-1}}$.

Expanding all the dependent variables $f(\mathbf{x}, t)$ as asymptotic series in powers of ε

$$f = f^{(0)} + \varepsilon f^{(1)} + \varepsilon^2 f^{(2)} + \cdots \qquad \text{(A9)}$$

leads to the dominant balance of (A8) at $O(\varepsilon^{-1})$:

$$(\mathbf{u}^{(0)})_h^{\perp} = -\nabla_h p^{(0)}, \quad \nabla_h \cdot \mathbf{u}_h^{(0)} = 0, \quad w^{(0)} = 0,$$
$$\frac{\partial p^{(0)}}{\partial z} = \frac{L_{du}}{L}(b_u^{(0)}H_u + b_s^{(0)}H_s). \qquad \text{(A10)}$$

Thus, the lowest-order pressure $p^{(0)}$ is a streamfunction $p^{(0)} = \psi$, with lowest-order horizontal velocity $\mathbf{u}_h^{(0)} = (u^{(0)}, \upsilon^{(0)})$, vorticity $\zeta^{(0)} = \partial\upsilon^{(0)}/\partial x - \partial u^{(0)}/\partial y$, and buoyancy given by, respectively,

$$u^{(0)} = -\frac{\partial\psi}{\partial y}, \quad \upsilon^{(0)} = \frac{\partial\psi}{\partial x}, \quad \zeta^{(0)} = \nabla_h^2\psi, \quad \text{and} \qquad \text{(A11a)}$$

$$b_u^{(0)}H_u + b_s^{(0)}H_s = \frac{L}{L_{du}}\frac{\partial\psi}{\partial z}. \qquad \text{(A11b)}$$

Using the nondimensional forms of the expressions for b_u and b_s given by (17), one finds the lowest-order buoyancy terms

$$b_u^{(0)} = \theta_e^{(0)} - q_t^{(0)} \quad (=\theta^{(0)} + q_v^{(0)} - q_v^{(0)} = \theta^{(0)}) \quad \text{and} \qquad \text{(A12a)}$$

$$b_s^{(0)} = \theta_e^{(0)} - q_{vs}(z) \quad [=\theta^{(0)} + q_{vs}(z) - q_{vs}(z) = \theta^{(0)}]. \qquad \text{(A12b)}$$

The lowest-order buoyancy is the potential temperature in both unsaturated and saturated regimes consistent with the assumption gQ/B in (A7). However, phase change information is nevertheless encapsulated in the different dependence on θ_e and q_t. As in the dry case, given the pressure $p^{(0)}$, the lowest-order FARE equations [(A10)–(A12)] diagnostically determine $(u^{(0)}, \upsilon^{(0)}, \theta^{(0)})$.

Now one may proceed to the next-order balances arising from (A8). The $O(1)$ balances of the continuity condition [(A8c)] and the curl of the horizontal momentum equation [(A8a)] lead to

$$\frac{D_h^{(0)}\zeta^{(0)}}{Dt} = \frac{\partial w^{(1)}}{\partial z}, \qquad \text{(A13)}$$

where $D_h^{(0)}/Dt = \mathbf{u}^{(0)}\cdot\nabla_h$. The $O(1)$ balances from (A8d) and (A8e) are, respectively,

$$\frac{D_h^{(0)}b_u^{(0)}}{Dt} + \frac{L_{du}}{L}w^{(1)} + V_r\frac{\partial q_r^{(0)}}{\partial z} = 0 \quad \text{and} \qquad \text{(A14a)}$$

$$\frac{D_h b_s^{(0)}}{Dt} + \frac{L_{ds}}{L}w^{(1)} = 0. \qquad \text{(A14b)}$$

Equations (A13) and (A14) are the PQG model in terms of the buoyancies b_u and b_s, and they are presented in the main text in dimensional form in (24).

As noted in the main text, consistency of (A12b), (A14b), and (22) requires an additional restriction on the change in anomalous saturation profile with altitude: $(dq_{vs}/dz)(d\tilde{q}_{vs}/dz)^{-1} = O(\varepsilon)$. This can be seen by comparing the form of N_s^2 that would arise as the asymptotic limit of (A4) and the form of N_s^2 that arises algebraically in moving from (22) to (24) and (25).

REFERENCES

Bannon, P., 1986: Linear development of quasi-geostrophic baroclinic disturbances with condensational heating. *J. Atmos. Sci.*, **43**, 2261–2274, doi:10.1175/1520-0469(1986)043<2261:LDOQGB>2.0.CO;2.

Brennan, M. J., and G. M. Lackmann, 2005: The influence of incipient latent heat release on the precipitation distribution of the 24–25 January 2000 U.S. East Coast cyclone. *Mon. Wea. Rev.*, **133**, 1913–1937, doi:10.1175/MWR2959.1.

Bretherton, C. S., 1987: A theory for nonprecipitating moist convection between two parallel plates. Part I: Thermodynamics and ''linear'' solutions. *J. Atmos. Sci.*, **44**, 1809–1827, doi:10.1175/1520-0469(1987)044<1809:ATFNMC>2.0.CO;2.

Charney, J. G., 1947: The dynamics of long waves in a baroclinic westerly current. *J. Meteor.*, **4**, 136–162, doi:10.1175/1520-0469(1947)004<0136:TDOLWI>2.0.CO;2.

——, 1948: On the scale of atmospheric motions. *Geofys. Publ.*, **17** (2), 1–17.

——, 1971: Geostrophic turbulence. *J. Atmos. Sci.*, **28**, 1087–1095, doi:10.1175/1520-0469(1971)028<1087:GT>2.0.CO;2.

Chen, S., and S. N. Stechmann, 2016: Nonlinear traveling waves for the skeleton of the Madden–Julian oscillation. *Commun. Math. Sci.*, **14**, 571–592, doi:10.4310/CMS.2016.v14.n2.a11.

Davis, C. A., 1992: A potential-vorticity diagnosis of the importance of initial structure and condensational heating in observed extratropical cyclogenesis. *Mon. Wea. Rev.*, **120**, 2409–2428, doi:10.1175/1520-0493(1992)120<2409:APVDOT>2.0.CO;2.

Deng, Q., L. M. Smith, and A. J. Majda, 2012: Tropical cyclogenesis and vertical shear in a moist Boussinesq model. *J. Fluid Mech.*, **706**, 384–412, doi:10.1017/jfm.2012.260.

De Vries, H., J. Methven, T. Frame, and B. Hoskins, 2010: Baroclinic waves with parameterized effects of moisture interpreted using Rossby wave components. *J. Atmos. Sci.*, **67**, 2766–2784, doi:10.1175/2010JAS3410.1.

Dias, J., and O. Pauluis, 2010: Impacts of convective lifetime on moist geostrophic adjustment. *J. Atmos. Sci.*, **67**, 2960–2971, doi:10.1175/2010JAS3405.1.

Eady, E. T., 1949: Long waves and cyclone waves. *Tellus*, **1** (3), 33–52, doi:10.3402/tellusa.v1i3.8507.

Emanuel, K. A., 1986: Some dynamical aspects of precipitating convection. *J. Atmos. Sci.*, **43**, 2183–2198, doi:10.1175/1520-0469(1986)043<2183:SDAOPC>2.0.CO;2.

——, M. Fantini, and A. J. Thorpe, 1987: Baroclinic instability in an environment of small stability to slantwise moist convection. Part I: Two-dimensional models. *J. Atmos. Sci.*, **44**, 1559–1573, doi:10.1175/1520-0469(1987)044<1559:BIIAEO>2.0.CO;2.

Evans, L., 1998: *Partial Differential Equations.* American Mathematical Society, 662 pp.

Frierson, D. M. W., A. J. Majda, and O. M. Pauluis, 2004: Large scale dynamics of precipitation fronts in the tropical atmosphere: A novel relaxation limit. *Commun. Math. Sci.*, **2**, 591–626, doi:10.4310/CMS.2004.v2.n4.a3.

——, I. M. Held, and P. Zurita-Gotor, 2006: A gray-radiation aquaplanet moist GCM. Part I: Static stability and eddy scale. *J. Atmos. Sci.*, **63**, 2548–2566, doi:10.1175/JAS3753.1.

Grabowski, W. W., and P. K. Smolarkiewicz, 1996: Two-time-level semi-Lagrangian modeling of precipitating clouds. *Mon. Wea. Rev.*, **124**, 487–497, doi:10.1175/1520-0493(1996)124<0487:TTLSLM>2.0.CO;2.

Held, I. M., and B. J. Soden, 2006: Robust responses of the hydrological cycle to global warming. *J. Climate*, **19**, 5686–5699, doi:10.1175/JCLI3990.1.

Hernandez-Duenas, G., A. J. Majda, L. M. Smith, and S. N. Stechmann, 2013: Minimal models for precipitating turbulent convection. *J. Fluid Mech.*, **717**, 576–611, doi:10.1017/jfm.2012.597.

——, L. M. Smith, and S. N. Stechmann, 2015: Stability and instability criteria for idealized precipitating hydrodynamics. *J. Atmos. Sci.*, **72**, 2379–2393, doi:10.1175/JAS-D-14-0317.1.

Hoskins, B. J., I. Draghici, and H. C. Davies, 1978: A new look at the ω-equation. *Quart. J. Roy. Meteor. Soc.*, **104**, 31–38, doi:10.1002/qj.49710443903.

Kessler, E., 1969: *On the Distribution and Continuity of Water Substance in Atmospheric Circulations. Meteor. Monogr.*, No. 32, Amer. Meteor. Soc., 84 pp.

Kuo, H. L., 1961: Convection in conditionally unstable atmosphere. *Tellus*, **13**, 441–459, doi:10.3402/tellusa.v13i4.9516.

Laliberté, F., T. Shaw, and O. Pauluis, 2012: Moist recirculation and water vapor transport on dry isentropes. *J. Atmos. Sci.*, **69**, 875–890, doi:10.1175/JAS-D-11-0124.1.

Lambaerts, J., G. Lapeyre, V. Zeitlin, and F. Bouchut, 2011: Simplified two-layer models of precipitating atmosphere and their properties. *Phys. Fluids*, **23**, 046603, doi:10.1063/1.3582356.

——, ——, and ——, 2012: Moist versus dry baroclinic instability in a simplified two-layer atmospheric model with condensation and latent heat release. *J. Atmos. Sci.*, **69**, 1405–1426, doi:10.1175/JAS-D-11-0205.1.

Lapeyre, G., and I. M. Held, 2004: The role of moisture in the dynamics and energetics of turbulent baroclinic eddies. *J. Atmos. Sci.*, **61**, 1693–1710, doi:10.1175/1520-0469(2004)061<1693:TROMIT>2.0.CO;2.

LeVeque, R. J., 2002: *Finite Volume Methods for Hyperbolic Problems.* Cambridge University Press, 578 pp.

Lin, Y.-L., R. D. Farley, and H. D. Orville, 1983: Bulk parameterization of the snow field in a cloud model. *J. Climate Appl. Meteor.*, **22**, 1065–1092, doi:10.1175/1520-0450(1983)022<1065:BPOTSF>2.0.CO;2.

Majda, A. J., and A. L. Bertozzi, 2002: *Vorticity and Incompressible Flow*. Cambridge Texts in Applied Mathematics, Vol. 27, Cambridge University Press, 545 pp.

——, and S. N. Stechmann, 2011: Nonlinear dynamics and regional variations in the MJO skeleton. *J. Atmos. Sci.*, **68**, 3053–3071, doi:10.1175/JAS-D-11-053.1.

——, Y. Xing, and M. Mohammadian, 2010: Moist multi-scale models for the hurricane embryo. *J. Fluid Mech.*, **657**, 478–501, doi:10.1017/S0022112010001515.

Mak, M., 1982: On moist quasi-geostrophic baroclinic instability. *J. Atmos. Sci.*, **39**, 2028–2037, doi:10.1175/1520-0469(1982)039<2028:OMQGBI>2.0.CO;2.

Monteiro, J., and J. Sukhatme, 2016: Quasi-geostrophic dynamics in the presence of moisture gradients. *Quart. J. Roy. Meteor. Soc.*, **142**, 187–195, doi:10.1002/qj.2644.

Newman, M., G. N. Kiladis, K. M. Weickmann, F. M. Ralph, and P. D. Sardeshmukh, 2012: Relative contributions of synoptic and low-frequency eddies to time-mean atmospheric moisture transport, including the role of atmospheric rivers. *J. Climate*, **25**, 7341–7361, doi:10.1175/JCLI-D-11-00665.1.

O'Gorman, P. A., 2011: The effective static stability experienced by eddies in a moist atmosphere. *J. Atmos. Sci.*, **68**, 75–90, doi:10.1175/2010JAS3537.1.

Pauluis, O., and J. Schumacher, 2010: Idealized moist Rayleigh-Benard convection with piecewise linear equation of state. *Commun. Math. Sci.*, **8**, 295–319, doi:10.4310/CMS.2010.v8.n1.a15.

——, and J. Dias, 2012: Satellite estimates of precipitation-induced dissipation in the atmosphere. *Science*, **335**, 953–956, doi:10.1126/science.1215869.

——, V. Balaji, and I. M. Held, 2000: Frictional dissipation in a precipitating atmosphere. *J. Atmos. Sci.*, **57**, 989–994, doi:10.1175/1520-0469(2000)057<0989:FDIAPA>2.0.CO;2.

Peixoto, J. P., and A. H. Oort, 1992: *Physics of Climate.* American Institute of Physics, 520 pp.

Pfahl, S., C. Schwierz, M. Croci-Maspoli, C. Grams, and H. Wernli, 2015: Importance of latent heat release in ascending air streams for atmospheric blocking. *Nat. Geosci.*, **8**, 610–614, doi:10.1038/ngeo2487.

Phillips, N. A., 1954: Energy transformations and meridional circulations associated with simple baroclinic waves in a two-level, quasi-geostrophic model. *Tellus*, **6**, 273–286, doi:10.1111/j.2153-3490.1954.tb01123.x.

Posselt, D. J., and J. E. Martin, 2004: The effect of latent heat release on the evolution of a warm occluded thermal structure. *Mon. Wea. Rev.*, **132**, 578–599, doi:10.1175/1520-0493(2004)132<0578:TEOLHR>2.0.CO;2.

Rhines, P. B., 1979: Geostrophic turbulence. *Annu. Rev. Fluid Mech.*, **11**, 401–441, doi:10.1146/annurev.fl.11.010179.002153.

Salmon, R., 1980: Baroclinic instability and geostrophic turbulence. *Geophys. Astrophys. Fluid Dyn.*, **15**, 167–211, doi:10.1080/03091928008241178.

Schneider, T., P. A. O'Gorman, and X. J. Levine, 2010: Water vapor and the dynamics of climate changes. *Rev. Geophys.*, **48**, RG3001, doi:10.1029/2009RG000302.

Schubert, W. H., S. A. Hausman, M. Garcia, K. V. Ooyama, and H.-C. Kuo, 2001: Potential vorticity in a moist atmosphere. *J. Atmos. Sci.*, **58**, 3148–3157, doi:10.1175/1520-0469(2001)058<3148:PVIAMA>2.0.CO;2.

Seifert, A., and K. D. Beheng, 2001: A double-moment parameterization for simulating autoconversion, accretion and selfcollection. *Atmos. Res.*, **59–60**, 265–281, doi:10.1016/S0169-8095(01)00126-0.

——, and ——, 2006: A two-moment cloud microphysics parameterization for mixed-phase clouds. Part 1: Model description. *Meteor. Atmos. Phys.*, **92**, 45–66, doi:10.1007/s00703-005-0112-4.

Seitter, K. L., and H.-L. Kuo, 1983: The dynamical structure of squall-line type thunderstorms. *J. Atmos. Sci.*, **40**, 2831–2854, doi:10.1175/1520-0469(1983)040<2831:TDSOSL>2.0.CO;2.

Shaw, T. A., and O. Pauluis, 2012: Tropical and subtropical meridional latent heat transports by disturbances to the zonal mean and their role in the general circulation. *J. Atmos. Sci.*, **69**, 1872–1889, doi:10.1175/JAS-D-11-0236.1.

Stechmann, S. N., and A. J. Majda, 2006: The structure of precipitation fronts for finite relaxation time. *Theor. Comput. Fluid Dyn.*, **20**, 377–404, doi:10.1007/s00162-006-0014-1.

Sutcliffe, R. C., 1947: A contribution to the problem of development. *Quart. J. Roy. Meteor. Soc.*, **73**, 370–383, doi:10.1002/qj.49707331710.

Trenberth, K. E., and D. P. Stepaniak, 2003: Covariability of components of poleward atmospheric energy transports on seasonal and interannual timescales. *J. Climate*, **16**, 3691–3705, doi:10.1175/1520-0442(2003)016<3691:COCOPA>2.0.CO;2.

Wetzel, A. N., L. M. Smith, and S. N. Stechmann, 2017: Moisture transport due to baroclinic waves: Linear analysis of precipitating quasi-geostrophic dynamics. *Math. Climate Wea. Forecasting*, submitted.